

See discussions, stats, and author profiles for this publication at: <https://www.researchgate.net/publication/245236069>

Kinetics of Desorption of 1,3Diisopropylbenzene and 1,3,5-Triisopropylbenzene. 1. Diffusion in Y-Zeolite Crystals by the Zero-Length-Column Method

ARTICLE in INDUSTRIAL & ENGINEERING CHEMISTRY RESEARCH · MARCH 2005

Impact Factor: 2.59 · DOI: 10.1021/ie049095u

CITATIONS

5

READS

155

3 AUTHORS, INCLUDING:



Sharif F Zaman

King Abdulaziz University

26 PUBLICATIONS 129 CITATIONS

SEE PROFILE



Sulaiman al-khattaf

King Fahd University of Petroleum and Miner...

117 PUBLICATIONS 1,118 CITATIONS

SEE PROFILE

Kinetics of Desorption of 1,3-Diisopropylbenzene and 1,3,5-Triisopropylbenzene. 1. Diffusion in Y-Zeolite Crystals by the Zero-Length-Column Method

Sharif F. Zaman,[†] Kevin F. Loughlin,* and Sulaiman S. Al-Khattaf[‡]

Department of Chemical Engineering, King Fahd University of Petroleum & Minerals, Dhahran 31261, Saudi Arabia

The kinetics of desorption of 1,3-diisopropylbenzene and 1,3,5-triisopropylbenzene from 0.9- μm NaY-zeolite crystals by the zero-length-column (ZLC) technique are reported. Both molecules were found to have nonlinear equilibrium adsorption properties because the observed K values are approximately 10^5 . Accordingly, the zero-loading diffusivities were extracted from the data using the nonlinear asymptotic form of the ZLC model. The desorption curve of 1,3-diisopropylbenzene was normal, but that of 1,3,5-triisopropylbenzene contained a discontinuity reminiscent of a percolation threshold. This was attributed to catalytic reaction, and the reported diffusivity for this material is hypothesized to be that of the codiffusion of diisopropylbenzene isomers with propylene. The reported activation energies are accordingly very similar for both species (≈ 66 and 77 kJ/mol, respectively); the activation energy for 1,3-diisopropylbenzene is intrinsic, whereas that for 1,3,5-triisopropylbenzene is a pseudo activation energy.

Introduction

1,3-Diisopropylbenzene and 1,3,5-triisopropylbenzene are frequently used as probe molecules to study the kinetics of reactions in catalysts for fluid catalytic cracking (FCC) processes instead of a complex mixture of oil molecules.^{1,2} The FCC catalysts are typically composed of Y zeolite in an alumina matrix and are widely used in hydrocarbon conversion processes because of their high activities and selectivities. The reaction kinetics of these catalysts are strongly influenced by both the zeolite crystal size and the intracrystalline diffusivity.³ The objective of this paper is to study the diffusion of 1,3-diisopropylbenzene and 1,3,5-triisopropylbenzene in Y-zeolite crystals to promote the understanding of the reaction kinetics of FCC processes.

There are limited studies of the diffusion of large molecules in faujasite-type materials, such as X or Y zeolite. Early studies were by Satterfield and co-workers^{4,5} and Moore⁶ primarily on the counterdiffusion of large molecules in the presence of cyclohexane in the liquid phase. The diffusivity values reported by Satterfield and co-workers appear to be smaller than those published in a later study by Culfaz and Ergun.⁷ Ruthven and Kaul⁸ suggested that effects other than intracrystalline diffusion may have been important in the earlier studies. Moore⁶ stated that the effective diffusion coefficient of the compact molecules (toluene, *p*-xylene, naphthalene, 1-methylnaphthalene, 1-ethylnaphthalene, 2-ethylnaphthalene, and mesitylene) correlates with the diameter of the smallest orifice through which the molecule can pass (the critical diameter), decreasing as the critical diameter increases. However, aromatic molecules with longer side chains, such as *m*-diisopropylbenzene or 1,3,5-triethylbenzene, deviate from this correlation perhaps because their structures

are more easily deformed. Further, such molecules with a critical diameter of 9.4 \AA readily diffuse in the pore structure with an orifice diameter of 7.4 \AA , although slowly. Ruthven and Kaul⁸ reported the diffusion of a range of aromatics [1,3,5-trimethylbenzene (mesitylene), 1,2,3,5-tetramethylbenzene, hexamethylbenzene, anthracene, and 1,3,5-triethylbenzene] in NaX zeolite. They confirmed the validity of the diffusion model for several of the sorbates and successfully correlated their diffusivity data with the moment of inertia of the sorbate molecule with one exception. Further, they showed a positive concentration dependence of diffusion for mesitylene and tetramethylbenzene in their figures and tabular results. Fujikata et al.⁹ reported that the diffusivities in the adsorption and desorption processes for aromatics and paraffins in Y-type zeolites were equal to each other when the pore size was larger than the molecule size. Hashimoto et al.¹⁰ measured the self-diffusivity of anthracene in Y zeolite using a triplet-triplet energy-transfer mechanism, found unconventional kinetics that could be modeled using continuous random walk theory, and obtained values of 10^{-15} – $10^{-16} \text{ m}^2/\text{s}$ at 298 K for the self-diffusivity. Cavalcante et al.¹¹ reported that the Fickian diffusion model was satisfactory in a study of linear paraffins (C_7 – C_{10}) in dealuminated USY zeolite using the zero-length-column (ZLC) method.

The specter of catalytic activity perturbs the measurement of diffusivities of large molecules. Ruthven and Kaul⁸ used an inactive sodium form of zeolite X but even still suggested that, in contact with the zeolite, triethylbenzene is slowly reacting. They also indicated that they suspect unnoticed catalytic activity in earlier diffusion measurements for triisopropylbenzene in NaX, which appeared to be too high when compared to the diffusivities of triethyl- or trimethylbenzene.¹² The literature is replete with references of catalytic cracking and coke formation for 1,3,5-triisopropylbenzene.^{3,13}

The ZLC technique developed by Eic and Ruthven¹⁴ is used in this study to measure intracrystalline diffu-

* To whom correspondence should be addressed. E-mail: lozhkf@kfupm.edu.sa.

[†] E-mail: zfscharif@chml.ubc.ca.

[‡] E-mail: skhattaf@kfupm.edu.sa.

sivities. Literature on the ZLC method is extensive. Theoretical intracrystalline models for diffusivity measurements are available for the linear isotherm region,¹⁴ nonlinear isotherm region,^{15,16} heat effects on ZLC experiments,^{17,18} and size distribution effects.¹⁹ Intracrystalline macropore diffusivity theories exist for linear isotherm regions.^{20,21} The theory for equilibrium isotherm determination for pure and binary systems has recently been developed.^{22,23} The ZLC method has also been extended to measure self-diffusion, counterdiffusion,^{24–26} liquid-phase diffusion measurements,^{27–29} and liquid-phase counterdiffusion.^{27–31}

In this study, we report on the investigation of the intracrystalline diffusion of 1,3-diisopropylbenzene and 1,3,5-triisopropylbenzene in Y-zeolite crystal by the ZLC method. Experimental data are fitted with the appropriate ZLC model equations to measure the diffusivities and activation energies for these hydrocarbons.

Mathematical Model

The ZLC, as originally developed by Eic and Ruthven,¹⁴ involved equilibration of a small sample of adsorbent at a known partial pressure of sorbate and then desorption with a helium purge. For uniform spherical adsorbent particles under linear equilibrium conditions, the response curve assuming Fickian diffusion and isothermal operation is given by³²

$$\frac{c}{c_0} = 2L \sum_{n=1}^{\infty} \frac{\exp\left(-\frac{\beta_n^2 D_0 t}{R^2}\right)}{\beta_n^2 + L(L-1)} \quad (1)$$

where β_n is given by the roots of the following equation:

$$\beta_n \cot \beta_n + L - 1 = 0 \quad (2)$$

$$L = \frac{1}{3} \frac{FR^2}{KV_s D} \quad (3)$$

L can be expressed as

$$L = \left(\frac{1}{3}\right) \left(\frac{\text{purge flow rate}}{\text{crystal volume}}\right) \left(\frac{R^2}{KD}\right) \quad (4)$$

In the long-time region, eq 1 reduces to a simple exponential decay curve because only the first term of the summation is significant:

$$\frac{c}{c_0} = \frac{2L}{\beta_1^2 + L(L-1)} \exp\left(-\frac{\beta_1^2 D_0 t}{R^2}\right) \quad (5)$$

Under these conditions, D_0/R^2 and L can be determined directly from the slope and intercept of the semilogarithmic plot of c/c_0 vs t . This is known as long-time (LT) analysis.

The assumption of linearity in the adsorption isotherm is generally not valid, especially when considering strongly adsorbed species. Brandani¹⁵ developed the model for ZLC experiments to analyze the effect of nonlinear equilibrium on the resulting apparent diffusivities assuming Langmuir equilibrium and the concentration dependence of zeolitic diffusivity varying according to Darken's relationship

$$D(q) = D_0 \frac{d \ln p}{d \ln q} = \frac{D_0}{1 - q/q_s} = \frac{D_0}{1 - \lambda Q} \quad (6)$$

where D_0 is the diffusivity at infinite dilution and q_s is the saturation loading. The extent of nonlinearity to a loading q_0 is described by the nonlinearity parameter $\lambda = q_0/q_s$ with $Q = q/q_0$ the dimensionless loading. A numerical solution was developed. The solution of these equations for the LT asymptote is given by

$$\ln \frac{c}{c_0} = \ln(1 - \lambda) - \lambda + \ln\left[\frac{2L}{\beta_1^2 + L(L-1)}\right] - \beta_1^2 \frac{D_0 t}{R^2} \quad (7)$$

If $\lambda \rightarrow 0$, the solution reduces to eq 5 as for the linear isotherm.

The intercept $\ln(1 - \lambda) - \lambda + \ln\{2L/[\beta_1^2 + L(L-1)]\}$ decreases because of an increase in the nonlinearity parameter λ , but the slope remains constant. If such curves are (incorrectly) analyzed on the basis of the linear model, the error in the value of D_0/R^2 will be minimal. However, the error in the apparent Henry's constant (derived from the intercept of eq 5) may be very large. From the practical point of view, Brandani¹⁵ came to the conclusion that nonlinearity affects the intercept of the $\ln(c/c_0)$ vs t plot (i.e., the equilibrium parameter K) but has little effect on the slope (i.e., the limiting diffusivity).

Apparatus, Materials, and Experimental Procedure

A schematic diagram of the ZLC apparatus is presented in Figure 1. The carrier gas (helium) is introduced in two streams and flow-controlled by mass flow controllers (manufactured by Omega Inc.). The ranges of the high and low mass flow controllers are 100 and 20 cm³/min, respectively. The low flow rate stream may be diverted to join the high flow rate stream directly or bubbled through a copper hydrocarbon chamber (liquid height 5 cm) in a water-temperature-controlled bath (20 °C) before rejoining the high flow rate stream. The height is sufficient to saturate the helium bubbles completely with hydrocarbon. The flow path is controlled by an on/off switch. The ZLC cell is made of a 1/4-in. stainless steel coupler, and the zeolite crystals are held between two sintered disks therein. To minimize the intrusion of thermal effects and/or extra particle resistance to mass transfer, the adsorbent quantity used is small, i.e., 1–10 mg. Tubing of 2 m in length is placed prior to the ZLC column inside the oven to provide the isothermal condition for gas flow. The outlet of the ZLC cell is connected to a flame ionization detector (FID), and the signal is recorded on a chart recorder.

The properties of Y-zeolite crystals, obtained from the Japanese Co. (TOESOH), are presented in Table 1 and for the hydrocarbons used in Table 2. The particle radius was determined by scanning electron microscopy (SEM); a typical scan is shown in Figure 2. The boiling points of the chemicals are above 200 °C, which suggests that isotherms will be highly nonlinear at extremely low pressures below this temperature. The molecular size given is the minimum kinetic critical diameter of these molecules for diffusion in a porous network.

For regeneration of the adsorbent, a small amount of crystal (2–10 mg) is heated in the ZLC cell at high temperature, i.e., 300–350 °C, for 16–18 h at a very low flow rate of the helium purge gas, i.e., 12–20 cm³/min.

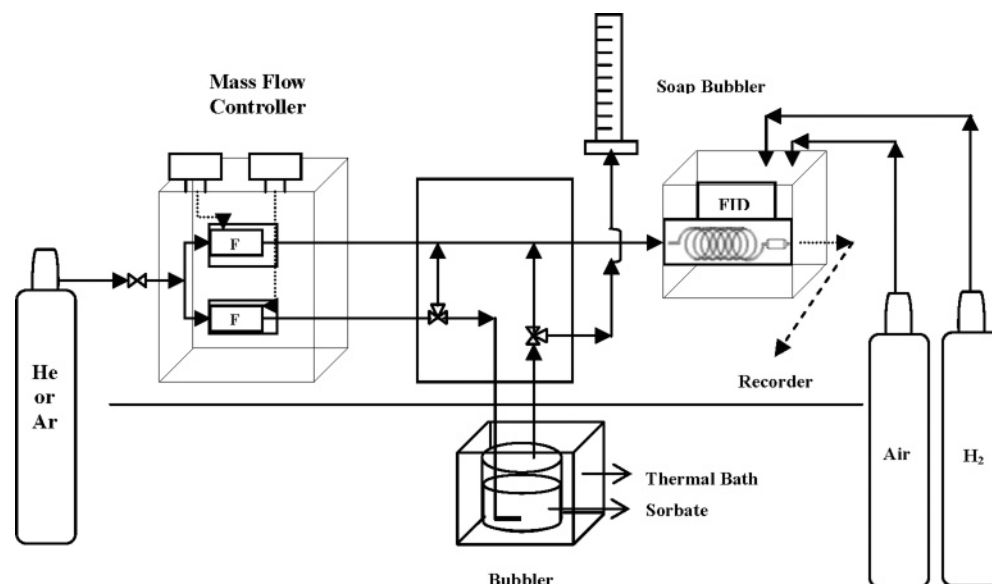


Figure 1. Schematic Diagram of experimental setup.

Table 1. Properties of a Y Catalyst

zeolite type ³⁶	faujasite
pore size (Å) ³⁶	7.4
BET surface area (m ² /g) ¹	583
hydrated density (g/cm ³) ³⁷	1.92
Na ₂ O (wt %) ¹	0.25
SiO ₂ /Al ₂ O ₃ (mol/mol) ¹	5.7
unit cell size (Å) ¹	24.51
crystal size (μm) ¹	0.9

Table 2. Properties of Hydrocarbons

hydrocarbon name	chemical formula	molecular weight	boiling point (°C) ^a	molecular size (Å)
1,3-diisopropylbenzene (3-isopropylcumene) ³⁵	C ₁₂ H ₁₈	162.28	210	8.4
1,3,5-triisopropylbenzene ³⁵	C ₁₅ H ₂₄	204.36	233	9.3

^a Boiling points are taken from the HYSYS software database.

After regeneration, the oven temperature is reduced to the desired temperature of the investigation and the high mass flow controller adjusted to a high value, i.e., 80–90 cm³/min. The low mass flow controller is adjusted to a low value, i.e., 8–10 cm³/min, and the helium flow rejoins the high mass flow controller output before entering the ZLC cell. The FID is started up, and sufficient time is allowed to locate a steady baseline on the recorder. The water bath is adjusted to the desired temperature (20 °C) to maintain the hydrocarbon bubbler temperature constant.

For adsorption, the low-flow-controlled stream is diverted to the liquid hydrocarbon bubbler, saturating the helium gas before rejoining the high mass flow for cell ZLC passage. This provides a very low hydrocarbon partial pressure in the gas stream (0.0297 and 0.002637 mmHg for 1,3-diisopropylbenzene and 1,3,5-triisopropylbenzene, respectively). Sufficient time is provided to achieve equilibrium of the zeolite crystals, observed via a constant recorder output.

For desorption, the low-mass-flow-controlled output is switched back to rejoin the high-flow helium flow rate prior to the bubbler, providing a pure helium purge. The concentration of hydrocarbon reduces with the time, and the data are recorded on the chart recorder. Again sufficient time to achieve a steady baseline for the complete desorption of adsorbed hydrocarbon is provided.

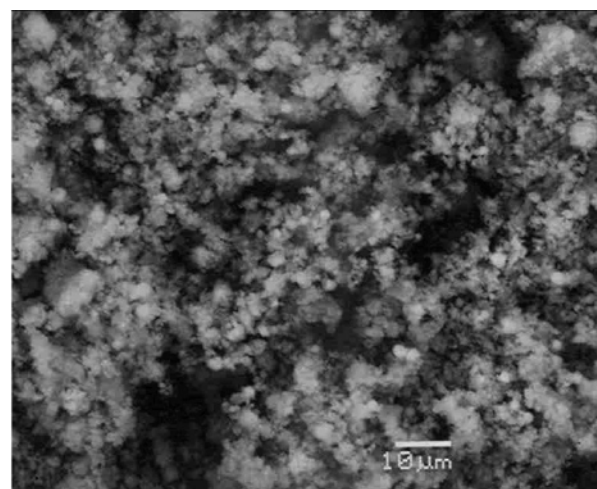


Figure 2. SEM analysis of a Y crystal.

Experiments were carried out at both 70 and 90 cm³/min flow rates to establish that measurements were in the kinetic regime. Similar diffusivities were calculated from both measurements, confirming the existence of the kinetic regime.

Results and Discussion

The adsorption step of 1,3-diisopropylbenzene was normal, rising as a smooth continuous curve from the zero baseline to equilibrium loading. For 1,3,5-triisopropylbenzene, the adsorption curve was initially smooth, but two discontinuities were observed at approximately 60 and 85% equilibration. Something irregular had happened during the adsorption that was not observed for any of the other sorbates tested.³³ Attempts to remove the discontinuities by varying the adsorption temperature failed. Catalytic activity occurring for this material was suspected as hypothesized by Ruthven et al.¹²

These molecules have minimum critical diameters (0.84 and 0.93 nm for 1,3-diisopropylbenzene and 1,3,5-triisopropylbenzene, respectively), which exceed the pore opening (0.74 nm) of the Y zeolite. The molecules are not rigid and must flex and bend to enter the Y zeolite, and significant steric hindrance must occur.

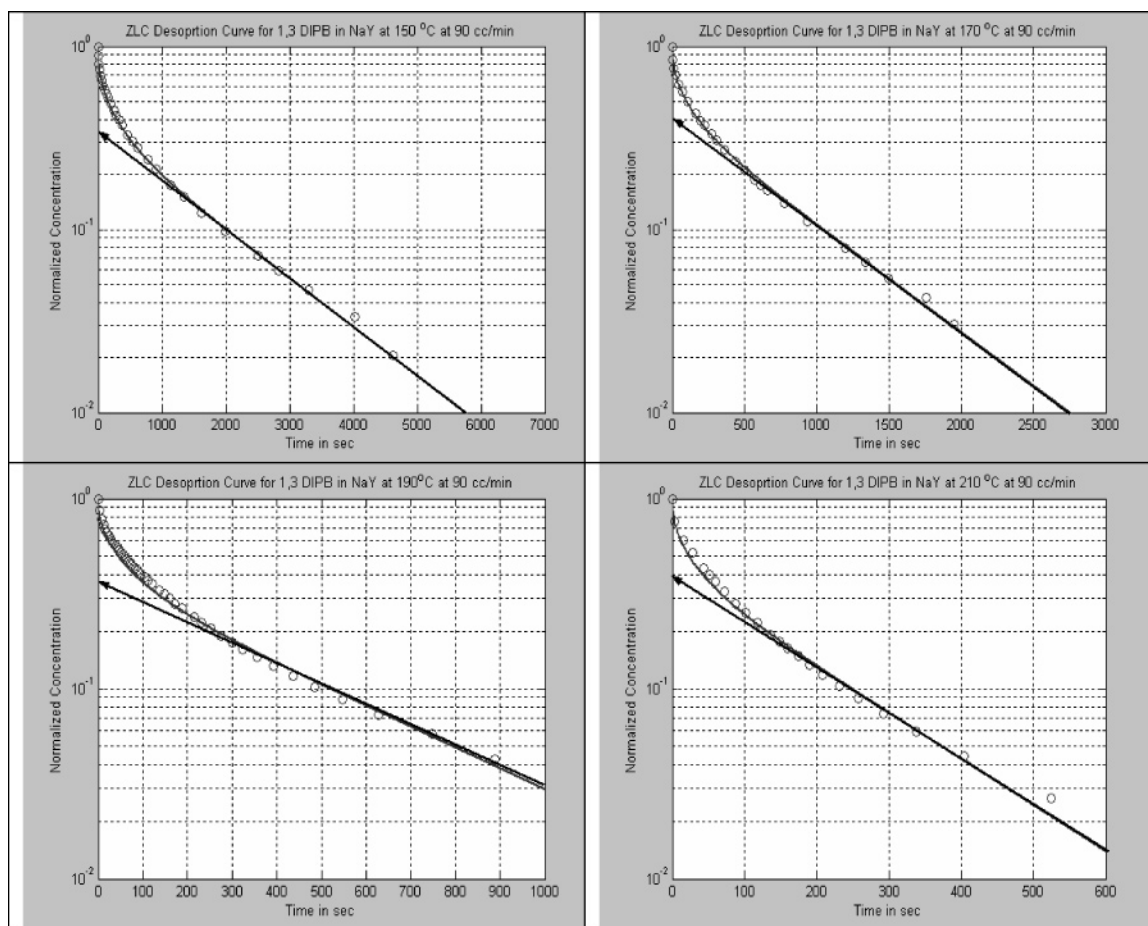


Figure 3. ZLC desorption curve for 1,3-diisopropylbenzene at 90 cm³/min for the temperature range of 150–210 °C.

Table 3. Diffusivity Values for the Hydrocarbon Molecules

hydrocarbon	temp (°C)	D/R^2 (s ⁻¹)	D (m ² /s)	D^* (m ² /s)	E (kJ/mol)	L	K
Data Results for 1,3-Diisopropylbenzene in a Y Zeolite							
1,3-diisopropylbenzene	150	8.35×10^{-5}	1.69×10^{-17}	3.00×10^{-9}	66.14	6.23	249 119.56
	170	2.06×10^{-4}	4.17×10^{-17}			4.61	136 287.37
	190	3.87×10^{-4}	7.84×10^{-17}			4.88	68 501.17
	210	9.08×10^{-4}	1.84×10^{-16}			4.46	31 939.09
Data Results for 1,3,5-Triisopropylbenzene in a Y Zeolite							
1,3,5-triisopropylbenzene	125	1.74×10^{-5}	3.53×10^{-18}	1.00×10^{-7}	77.74	14.14	595 142.80
	150	8.35×10^{-5}	1.69×10^{-17}			6.56	286 552.25
	170	3.14×10^{-4}	6.35×10^{-17}			5.47	91 579.29
	190	1.13×10^{-3}	2.30×10^{-16}			3.69	22 627.97
	75	4.87×10^{-5}	9.87×10^{-18}			8.81	
	125	7.75×10^{-5}	1.57×10^{-17}			10.2	
	150	4.46×10^{-4}	9.04×10^{-17}			3.56	

Desorption plots for 1,3-diisopropylbenzene are presented in Figure 3, and the optimized experimental parameter values are tabulated in Table 3. The investigation temperature range is 150–210 °C. The data were first analyzed using the linear ZLC model. Apparent values of L and K , calculated by eqs 5 and 3, respectively, are reported in Table 3. Apparent L values ranged from 4.46 to 6.23, satisfactory for the evaluation of kinetic data, and apparent K values ranged from 31 939 to 249 119. Because these are in the nonlinear range, eq 7 was used to calculate the diffusivities, and these are the values reported. This is the straight line shown on the plots. Further, because we did not have isotherm data for this hydrocarbon, it was not possible to calculate the λ value and, hence, the degree of approach to saturation. However, with these high apparent K values, the degree of approach is expected to be high, possibly exceeding 90%. Further, it was not

possible to calculate the actual L values because we lacked the true λ value. Also shown in the figures is the solution of the dimensionless linear ZLC model using the apparent values of L and K . As may be observed, the fit in the LT region is excellent. Diffusivity values are approximately 10^{-17} m²/s. Moore and Katzer⁵ reported that the diffusivity value at 25 °C is around 2×10^{-17} m²/s, and this value is higher than our experimental results.

Desorption plots for 1,3,5-triisopropylbenzene are presented in Figures 4–6, and the optimized experimental values are tabulated in Table 3. The temperature range of the investigation is 75–190 °C.

Diffusivity values for the runs at 125 and 150 °C have diffusivity values varying by up to a factor of 4. In fact, the three runs at 75, 125, and 150 °C had longer initiation periods (shown in Figure 6) than the other runs. This may be attributable to different time spans

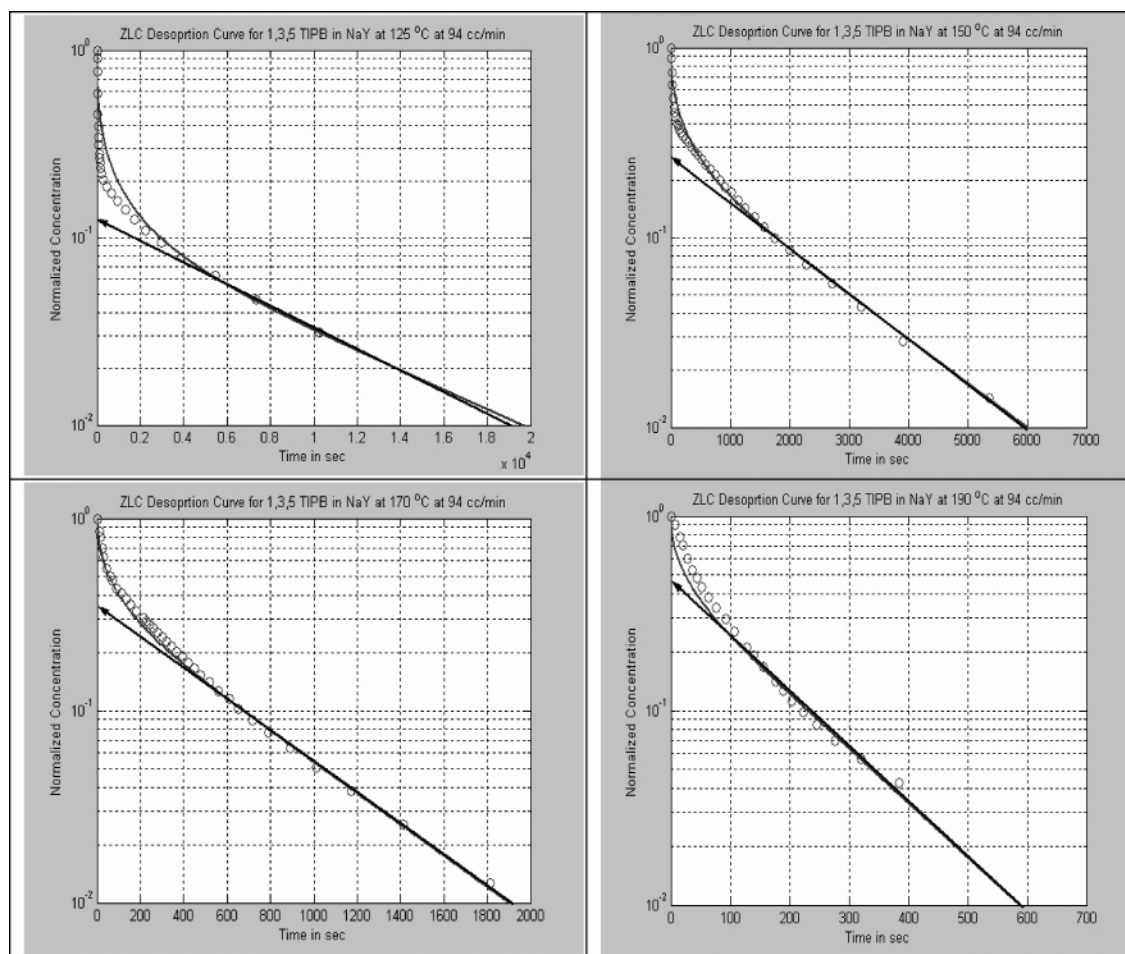


Figure 4. ZLC desorption curve for 1,3,5-triisopropylbenzene at 94 cm³/min for the temperature range of 125–190 °C.

of the adsorption step, resulting in unexpected coking, which may have affected the diffusion step. Normally, the time span of the adsorption step is not a consideration in measuring the desorption diffusivity by the ZLC method, and this is probably true in 99% of the runs. In the case of reaction and coking, this is a consideration and the time span for the adsorption step needs to be carefully monitored. This concept did not come to light until the review of this study; it will be carefully monitored in any future work.

All of the plots contained a discontinuity in the initial region of desorption. Figure 6 is an expanded view of this region, indicating probably two different diffusion regimes. Initially, we have a slow desorption curve, which after some time (approximately 50 s) reaches a percolation threshold and becomes more rapid.

Two possible explanations of this phenomenon follow. The first hypothesis is that 1,3,5-triisopropylbenzene is not at all successful in penetrating inside the zeolite pores. It just adsorbs on the surface of the zeolite, only 3% of the total area available, because most of the adsorbed area is inside the zeolite pores. However, this would give a much faster desorption initially, which is contrary to what is observed. The second postulate is that reaction occurs in the catalytic adsorbent. Initially, we have a desorption curve that is controlled by the slow diffusion rate of unreacted 1,3,5-triisopropylbenzene. The unreacted material is postulated to occupy the outer shell of the crystal. In the interior of the crystal, all of 1,3,5-triisopropylbenzene is believed to have reacted to produce isomers of diisopropylbenzene and propylene,

and it is postulated that there is no more unreacted material in the central core. As soon as the ZLC is switched to desorption, the desorption rate is controlled by the outer shell, where the majority of the unreacted 1,3,5-triisopropylbenzene resides. In this outer shell, three phenomena are presumed to occur simultaneously. These are (1) diffusion of 1,3,5-triisopropylbenzene out of the crystal, (2) diffusion of 1,3,5-triisopropylbenzene into the crystal interior from the outer shell due to the existence of a concentration gradient because the central core lacks any of this material due to reaction, and (3) reaction of 1,3,5-triisopropylbenzene to produce isomers of diisopropylbenzene and propylene. The diffusivity in the first 50 s is then probably controlled by the diffusion of 1,3,5-triisopropylbenzene even if there are other molecules diffusing through the outer shell because the diffusion rates of these other molecules are controlled by the presence of a larger slower moving species. Thereafter, when the majority of 1,3,5-triisopropylbenzene has reacted in the outer shell, the diffusion reaches a percolation threshold because the diffusing molecules will be the product of reaction, which are the isomers of diisopropylbenzene and propylene. We will have codiffusion of these two molecules out of the crystal probably in the nonlinear region. The measured flux of 1,3-diisopropylbenzene, J_1 , is due to the chemical potential gradient of both molecules^{38,39} given by

$$J_1 = -D\nabla q \quad (8)$$

where \mathbf{D} is the first row of the matrix of coefficients and

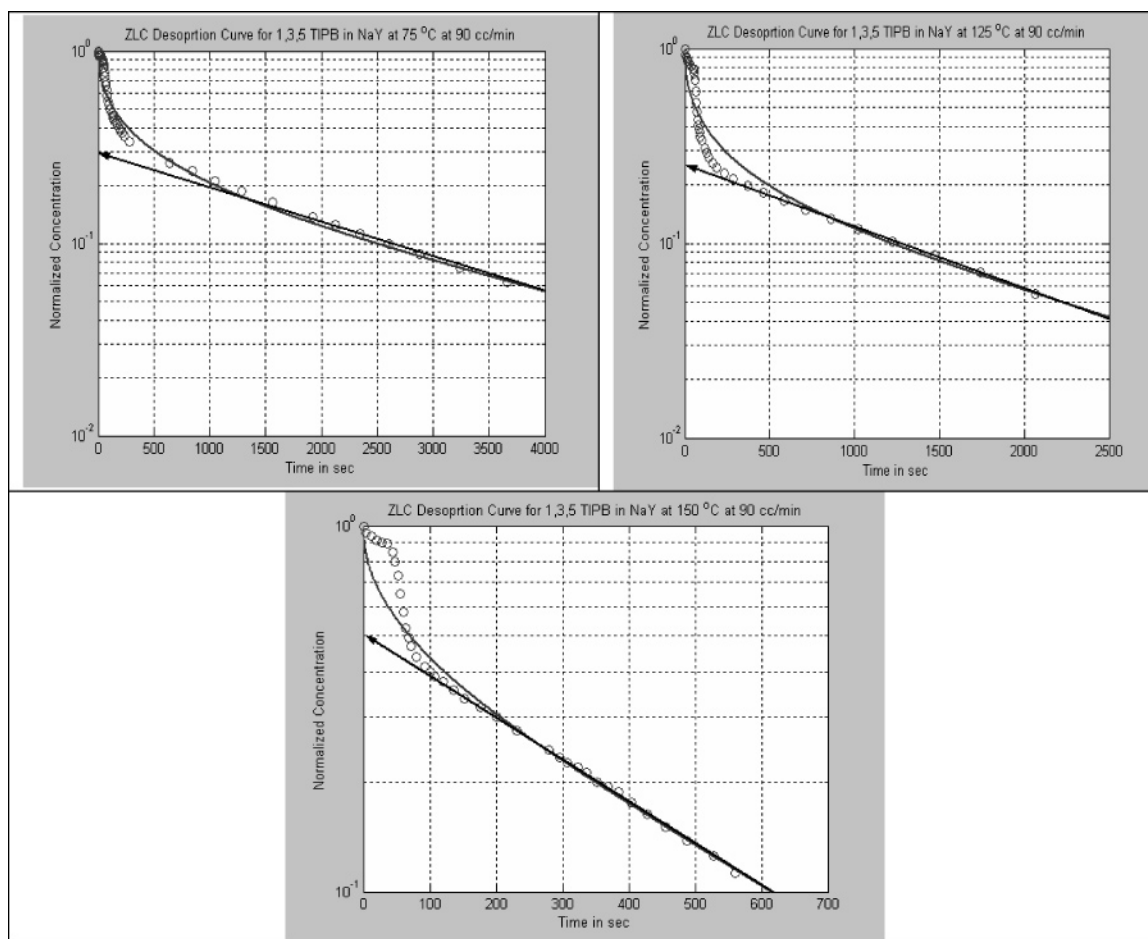


Figure 5. ZLC desorption curve for 1,3,5-triisopropylbenzene at 90 cm³/min for the temperature range of 75–125 °C.

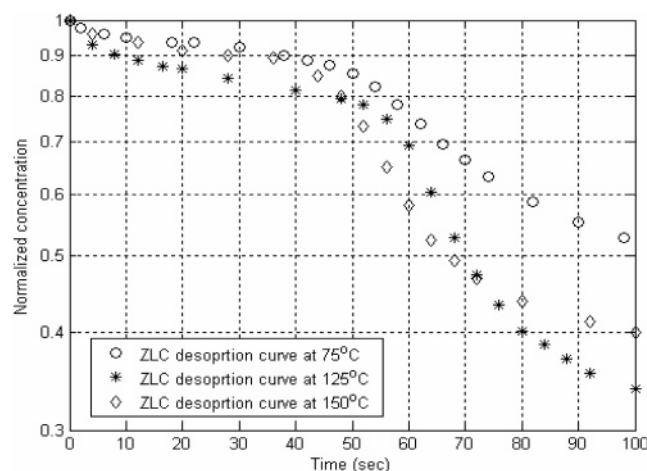


Figure 6. Expanded view of the initial region of the desorption curve for 1,3,5-triisopropylbenzene. The flow rate is 90 cm³/min.

is a function of loading [θ_1, θ_2], hopping rates of different species [q_1, q_2], and the distance between intersections [α] as per the arguments of Qureshi and Wei,³⁹ i.e.

$$\mathbf{D} = f(\alpha, q_1, q_2, \theta_1, \theta_2) \quad (9)$$

However, the experimental measurement that is usually made is that of an apparent diffusion coefficient given by

$$D_{\text{app}} = -J_i / \nabla \theta_i \quad (10)$$

D_{app} then is a contribution of driving forces, concentrations, and hopping rates. This is what is reported in this study because the intrinsic parameters are not known. The reported diffusivity values of the LT nonlinear asymptotic solution of the ZLC model for 1,3,5-triisopropylbenzene thus appear to be for the codiffusion of isomers of diisopropylbenzene and propylene and are expected to be greater than the single-component diffusivity of 1,3-diisopropylbenzene on its own.

It is not possible to estimate the diffusivity at the initial time region for two reasons at present. The first reason is that this is the region that is controlled by the time constant of the apparatus as a result of dead-volume limitations and so forth. The second reason is that the system is highly nonlinear, and the nonlinear solution parameter λ concerning the equilibrium loading is unknown, so that we cannot apply the nonlinear model of Brandani.¹⁵ Further, because it is probably a mixture of hydrocarbons, it will be difficult to calculate at any time. We solved the linear ZLC model using orthogonal collocation in this region and found the diffusivities to be a factor of 3–6 times lower than those for the asymptotic nonlinear solution, but the values of L obtained were complex. It was the latter result that directed us to the nonlinear aspects of the solution.

A discontinuity somewhat similar in effect to the one reported here has been observed by Brandani et al.²⁵ while studying the countercurrent diffusion in a ZLC apparatus of *p*-xylene (desorbing, smaller molecule) and *o*-xylene (adsorbing, larger kinetic diameter molecule) in large silicalite crystals. They opine that *o*-xylene cannot be accurately described by the diffusion model.

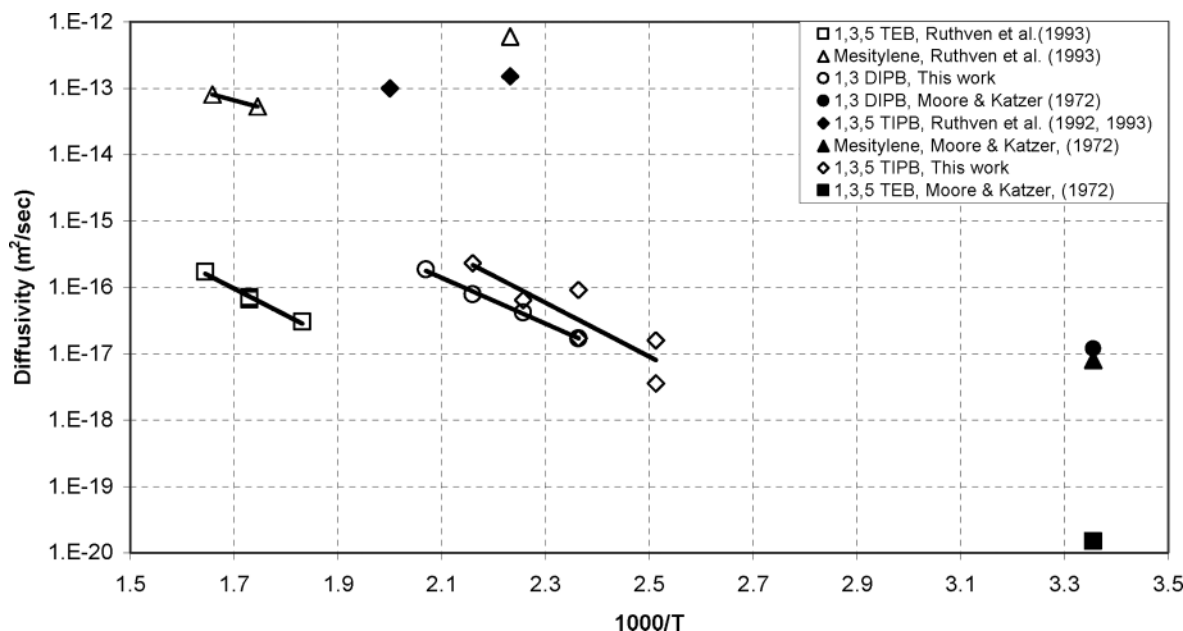


Figure 7. Arrhenius plot for 1,3-diisopropylbenzene and 1,3,5-triisopropylbenzene in a Y crystal.

For *p*-xylene, they observed an abrupt drop in the concentration after about 25 s, which they attributed to be reminiscent of a percolation threshold. The complex counterdiffusion of *p*-xylene appears to have three regimes: an initial slow desorption (to $c/c_0 \approx 0.7$), a transition at the percolation threshold to a faster desorption regime ($0.7 > c/c_0 > 0.05$), and a further slow desorption to zero loading below that observed in normal ZLC probably because of the presence of the counterdiffusing molecule. An explanation for why the *p*-xylene molecule passed through a percolation threshold is not clear. The first two effects are quite similar to the observations in this work, with a larger molecule incoming initially and smaller molecules exiting. Because there is no large molecules incoming at long time in this work, the last regime observed by Brandani et al.²⁶ does not exist.

The question arises as to when the percolation threshold occurs in this work. Ruthven,³⁴ in a study of diffusion in 4A and 5A zeolites, found that the system reached a percolation threshold when about 33% of the sodium ions were replaced by calcium ions. At that stage, the 4A structure had opened up sufficiently for the system to behave like a 5A zeolite, with sufficient passages available for the larger molecules to transit as if through a 5A zeolite. Using this analogy, it is postulated that when the concentration of 1,3,5-triisopropylbenzene reaches 66.6% in the outer shell, sufficient passages are available for the diisopropylbenzene isomers to exit as if 1,3,5-triisopropylbenzene is no longer limiting the diffusivity. A Monte Carlo simulation is probably needed to establish this hypothesis.

We report the diffusivities at long time and for zero loading conditions for 1,3,5-triisopropylbenzene, but as mentioned above, the reported diffusivity values of the LT nonlinear asymptotic solution of the ZLC model for this material appear to be for the codiffusion of isomers of diisopropylbenzene and propylene. It should be noted that 1,3,5-triisopropylbenzene is a big molecule and may even have structural instability above 150 °C in the gas phase. Using the linear ZLC model, apparent L values ranging from 3.69 to 14.14, satisfactory for kinetic measurements, and apparent K values ranging from

22 627 to 595 142 were calculated. Because these are in the nonlinear range, eq 7 was used to calculate the diffusivities, and these are the values reported. The diffusivity values reported from the experiment are in the range of 10^{-16} – 10^{-18} m^2/s . The fit of the nonlinear straight-line asymptotic solution and the linear ZLC using the parameters in Table 3 is shown in Figures 4 and 5.

One other point worth mentioning is that the cracking of the 1,3,5-triisopropylbenzene molecule should result in coke formation, and indeed this was observed in the zeolites after each experiment. This should result in slow diffusion in the codiffusion of the diisopropylbenzene isomers and propylene because of some pore blockage and may have occurred in some of the runs. The hypothesis that 1,3,5-triisopropylbenzene is reacting may be tested by adding a gas chromatograph–mass spectrometer system to the ZLC output in place of the FID analysis to analyze the contents of the gas stream. Also, an accurate measurement of any coke formed may be determined by a Multi EA 2000 to an accuracy of better than 0.1%. Both concepts are in our future plans.

The last question that arises concerns the possibility of measuring the diffusivity of 1,3,5-triisopropylbenzene in Y zeolite. It is doubtful whether this can be done gravimetrically, volumetrically, or by NMR because a quick-response instrument is required in the initial uptake region. It may be possible to do it using the ZLC technique, providing the entire adsorption curve (with its mass-transfer limitations), and the desorption curve with its slow and percolation regions is modeled. The main problems are the determination of the nonlinear isotherm and the limitations imposed by the dead volumes in the ZLC. The possibility of using other fast-response instruments needs to be explored.

Activation Energy Determination

Diffusion in zeolite is an activated process, described by the Eyring equation $D = D_0 e^{-E/RT}$. The data are plotted in Figure 7 together with known data mainly for NaX from the literature. The calculated activation energies and preexponential factors are 66.14 and 77.74

Table 4. Literature Value of Hydrocarbon Diffusivity in NaX

hydrocarbon name	crystal size (μm)	temp ($^{\circ}\text{C}$)	diffusivity (m^2/s)	D^* (m^2/s)	activation energy (kcal/mol)	method	ref
1,3-diisopropylbenzene (8.4 Å)		25	1.20×10^{-17}				Moore and Katzer ⁵
mesitylene (8.4 Å)	55	175	6.00×10^{-13}		25	gravimetric	Karger and Ruthven ³⁵
	100	300	6.25×10^{-14}				Ruthven and Kaul ⁸
	100	330	8.30×10^{-14}				
1,3,5-triethylbenzene (9.2 Å)	30, 50	273	3.00×10^{-17}	6.00×10^{-10}	76	gravimetric	Ruthven and Kaul ⁸
		305	7.00×10^{-17}				
		305	6.50×10^{-17}				
		335	1.70×10^{-16}				
		25	1.50×10^{-20}				Moore and Katzer ⁵
1,3,5-triisopropylbenzene (9.4 Å)	x	227	1.00×10^{-13}			gravimetric	Ruthven et al. ¹²
	55	175	1.50×10^{-13}		58	gravimetric	Karger and Ruthven ³⁵

kJ/mol and 3×10^{-9} and 1×10^{-7} m^2/s for 1,3-diisopropylbenzene and 1,3,5-triisopropylbenzene, respectively. The higher activation energy for 1,3,5-triisopropylbenzene above the diffusion for 1,3-diisopropylbenzene is probably a pseudo activation energy resulting from the codiffusion of both 1,3-diisopropylbenzene and propylene. It is not clear how the interaction of these two species affects the overall measured pseudo activation energy presumed to be that for 1,3-diisopropylbenzene alone. The diffusivities of 1,3,5-triisopropylbenzene are above the diffusivities of 1,3-diisopropylbenzene. This is consistent with the hypothesis advanced above that the diffusivities reported here are those of the codiffusing molecules of the isomers of diisopropylbenzene and propylene. The isomers of diisopropylbenzene formed should probably be 1,3 if we allow for the shearing of one isopropyl group with no rearrangement of the other groups. Thus, the diffusivities should probably be the same as those of 1,3-diisopropylbenzene. The reason they are higher is probably due to the combined driving force of the two molecules, increasing the flux out of the system. Alternatively, it could be due to the formation of 1,4-diisopropylbenzene in the cracking reaction, and this molecule should diffuse faster. Further, it is evident that the minute quantities of coke formed in the reaction do not appear to have hindered the diffusion of these two products because the diffusivities are greater than those for 1,2-diisopropylbenzene. However, the absolute diffusivity values may have been affected by the presence of different amounts of coke.

For NaX, Karger and Ruthven³⁵ reported the value of E for 1,3,5-triisopropylbenzene as around 58 kJ/mol. Mesitylene has the same kinetic diameter as 1,3-diisopropylbenzene, and diffusivity is reported by Ruthven and Kaul.⁸ If we extrapolate the diffusivity values, we can see that mesitylene has lower diffusivity values than 1,3-diisopropylbenzene. Mesitylene has three methyl groups at the 1, 3, and 5 positions and thus should have less rotational flexibility than 1,3-diisopropylbenzene. Possibly it may bend and thus deform its structure to diffuse more easily through the pores. 1,3,5-Triethylbenzene, which has the same critical molecular diameter as 1,3,5-triisopropylbenzene, has a much lower diffusivity than 1,3,5-triisopropylbenzene. This may be due to the fact that it does not decompose as rapidly as 1,3,5-triisopropylbenzene. Values of diffusivity reported by earlier works are tabulated in Table 4 and are displayed in the Arrhenius plot for comparison. The value of the diffusivity of 1,3,5-triisopropylbenzene of Moore and Katzer⁵ appears to be close to an extrapolation of the data for this work.

Conclusions

The diffusivities of 1,3-diisopropylbenzene and 1,3,5-triisopropylbenzene in a Y-zeolite crystal as measured by the ZLC technique are reported. The desorption systems are observed to be nonlinear, and the asymptotic form of the nonlinear ZLC model is used to extract the diffusivities. The desorption of 1,3,5-triisopropylbenzene produces a discontinuity in its desorption curve, and this is explained as a percolation threshold due to a catalytic cracking mechanism. The diffusivities measured are hypothesized to be the cracking products of this reaction. Activation energies are also reported. These values can be used in the modeling of cracking reactions.

Acknowledgment

The authors acknowledge the support of King Fahd University of Petroleum & Minerals (Project SABIC/2003-13) during the course of this work and the preparation of this paper.

Nomenclature

- c = fluid-phase sorbate concentration (mol/m^3)
- c_0 = initial fluid-phase sorbate concentration (mol/m^3)
- D = intracrystalline diffusion coefficient (m^2/s)
- D_0 = corrected diffusivity, defined by eq 6 (m^2/s)
- D^* = preexponential factor in the Eyring equation (m^2/s)
- D_{app} = apparent diffusion coefficient for mixture desorption (m^2/s), defined by eq 10
- \mathbf{D} = matrix of two-component diffusion
- F = volumetric fluid flow of the purge fluid (cm^3/min)
- J_i = flux of species i defined by eq 9
- K = dimensionless Henry's adsorption constant
- L = dimensionless ZLC parameter
- q = adsorbed-phase sorbate concentration (mol/m^3)
- q_0 = sorbate concentration in equilibration with c_0 (mol/m^3)
- q_s = saturated sorbate concentration (mol/m^3)
- q_i = hopping rate of a molecule to a specific adjacent site
- Q = dimensionless loading
- r = radial position within the sorbent particle (m)
- R = sorbent particle radius (m)
- t = time (s)
- V_s = volume of the solid (m^3)
- α = distance between intersections on a two-dimensional grid
- β = roots of eq 3.5
- θ_i = occupancy of the component
- λ = isotherm nonlinearity parameter

Literature Cited

- (1) Al-Khattaf, S.; de Lasa, H. I. The Role of Diffusion in Alkyl-Benzenes Catalytic Cracking. *Appl. Catal. A* **2000**, 226 (1–2), 139–153.
- (2) Al-Khattaf, S.; de Lasa, H. I. Catalytic Cracking of Alkyl-Benzene in a Novel CREC Riser Simulator—Effects of Y-Zeolite Crystal Size. In *Fluid Catalytic Cracking V, Studies in Surface Science and Catalysis*; Occelli, M. L.; O'Connor, P. O., Eds.; Elsevier: New York, Apr 2001; Vol. 134, pp 279–292.
- (3) Al-Khattaf, S.; Atias, A. J.; de Lasa, H. I. Diffusion and Catalytic Cracking of 1,3,5 tri-isopropyl benzene in FCC Catalysis. *Chem. Eng. Sci.* **2000**, 57 (22–23), 4909–4920.
- (4) Satterfield, C. N.; Katzer, J. R. Counterdiffusion of Liquid Hydrocarbons in Type Y Zeolites. *Adv. Chem. Ser.* **1971**, 193–208.
- (5) Moore, R. M.; Katzer, J. R. Counter diffusion of liquid hydrocarbons in type Y zeolite. Effect of molecular size, molecular type and diffusion direction. *AIChE J.* **1972**, 18, 816–824.
- (6) Moore, R. M. Counter diffusion of Liquid Hydrocarbons in the type Y Zeolite. Effect of Molecular Size, Shape and Type. *Chem. Eng. J.* **1971**, 6, 38–42.
- (7) Culfaz, A.; Ergun, G. Counterdiffusion of liquid hydrocarbon pairs in ion-exchanged forms of zeolite X. *Sep. Sci. Technol.* **1986**, 21 (5), 495–517.
- (8) Ruthven, D. M.; Kaul B. K. Adsorption of aromatic hydrocarbons in NaX zeolite. 2. Kinetics. *Ind. Eng. Chem. Res.* **1993**, 32, 2053–2057.
- (9) Fujikata, Y.; Masuda, T.; Ikeda, H.; Hasimoto, K. Measurement of the diffusivities with MIF and Y type zeolite catalysts in adsorption and desorption processes. *Microporous Mesoporous Mater.* **1998**, 21 (4–6), 679–686.
- (10) Hashimoto, S.; Hagiri, M.; Barzykin, A. V. Triplet–Triplet Energy Transfer as a Tool for Probing Molecular Diffusivity within Zeolites. *J. Phys. Chem. B* **2002**, 106 (4), 844–852.
- (11) Cavalcante, C. L., Jr.; Silva, N. M.; Souza, E. F.; Sobrinho, E. V. Diffusion of paraffins in dealuminated Y mesoporous molecular sieve. *Adsorption* **2003**, 9, 205–212.
- (12) Ruthven, D. M.; Eic, M.; Xu, Z. Diffusion of Hydrocarbons in A and X Zeolites and Silicalite. In *Catalysis and Adsorption by Zeolites*; Ohlmann, G., Pfeifer, H., Ficke, R., Eds.; Elsevier: Amsterdam, The Netherlands, 1991; pp 233–246.
- (13) S-Aguiar, E. F.; Murta-Valle, M. L.; Cardoso, D. Cracking of 1,3,5-triisopropylbenzene over deeply dealuminated Y zeolite. *Stud. Surf. Sci. Catal.* **1995**, 97, 417–422.
- (14) Eic, M.; Ruthven, D. M. A New Experimental Technique for Measurement for Intracrystalline Diffusivity. *Zeolites* **1988**, 8, 40–45.
- (15) Brandani, S. Effects of Nonlinear Equilibrium on Zero Length Column Experiments. *Chem. Eng. Sci.* **1998**, 53 (15), 2719–2798.
- (16) Brandani, S.; Jama, M. A.; Ruthven, D. M. ZLC Measurement Under Nonlinear Conditions. *Chem. Eng. Sci.* **2000**, 55 (7), 1205–1212.
- (17) Brandani, S.; Cavalcante, C. L.; Guimaraes, L.; Ruthven, D. M. Heat Effects in ZLC Experiments. *Adsorption* **1998b**, 4, 275–285.
- (18) Silva, J. A. C.; Da Silva, F. A.; Rodrigues, A. E. An Analytical Solution for the Analysis of Zero-Length-Column Experiments with Heat Effects. *Ind. Eng. Chem. Res.* **2001**, 40 (16), 3697–3702.
- (19) Duncan, W. L.; Moller, K. P. The Effect of a Crystal Size Distribution on ZLC Experiments. *Chem. Eng. Sci.* **2002**, 57 (14), 2641–2652.
- (20) Brandani, S. Analytical Solution for ZLC Desorption Curves with Bi-Porous Adsorbent Particle. *Chem. Eng. Sci.* **1996**, 51 (12), 3283–3288.
- (21) Silva, J. A. C.; Rodrigues, A. E. Analysis of ZLC Technique for Diffusivity Measurement in Bidisperse Porous Adsorbent Pellets. *Gas Sep. Purif.* **1996**, 10 (4), 207–224.
- (22) Brandani, F.; Ruthven, D. M.; Coe, C. G. Measurement of Adsorption Equilibrium by Zero Length Column (ZLC) Technique. Part 1: Single Component Systems. *Ind. Eng. Chem. Res.* **2003**, 42 (7), 1451–1461.
- (23) Brandani, F.; Ruthven, D. M.; Coe, C. G. Measurement of Adsorption Equilibrium by Zero Length Column (ZLC) Technique. Part 2: Binary Systems. *Ind. Eng. Chem. Res.* **2003**, 42 (7), 1462–1469.
- (24) Brandani, S.; Ruthven, D. M. Analysis of ZLC Desorption Curves. *Adsorption* **1996**, 2, 133–143.
- (25) Brandani, S.; Jama, M. A.; Ruthven, D. M. Counterdiffusion of *p*-xylene/*o*-xylene in silicalite Studied by Zero Length Column. *Ind. Eng. Chem. Res.* **2000**, 39 (3), 821–828.
- (26) Brandani, S.; Jama, M. A.; Ruthven, D. M. Diffusion, Self-Diffusion and Counterdiffusion of Benzene and *p*-Xylene in Silicalite. *Microporous Mesoporous Mater.* **2000**, 35 (6), 283–300.
- (27) Brandani, S.; Ruthven, D. M. Analysis of ZLC Desorption Curves for Liquid Systems. *Chem. Eng. Sci.* **1995**, 50, 2055–2059.
- (28) Boulicaut, L.; Brandani, S.; Ruthven, D. M. Liquid-Phase Sorption of Branched and Cyclic Hydrocarbons in Silicalite. *Microporous Mesoporous Mater.* **1998**, 25, 81–93.
- (29) Rodriguez, J. F.; Valverde, J. L.; Rodrigues, A. E. Measurement of Effective Self-Diffusion Coefficients in a Gel-Type Cation Exchanger by the Zero Length Column Method. *Ind. Eng. Chem. Res.* **1998**, 37, 2020–2028.
- (30) Chertontonghai, P.; Brandani, S. Liquid-phase counter-diffusion of aromatics in silicalite using ZLC method. *Adsorption* **2003**, 9, 197–204.
- (31) Ruthven, D. M.; Stapleton, P. Measurement of Liquid-Phase Counter Diffusion in Zeolite Crystals by ZLC Method. *Chem. Eng. Sci.* **1993**, 48 (1), 89–98.
- (32) Crank, J. *The mathematics of diffusion*, 1st ed.; Oxford University Press: London, 1956.
- (33) Zaman, S. F. Diffusion and Adsorption of Aromatics in Zeolites by Zero Length Column Technique. M.S. Thesis, Department of Chemical Engineering, King Fahd University of Petroleum & Minerals, Dhahran, Saudi Arabia, 2004.
- (34) Ruthven, D. M. Diffusion in Partially Ion Exchanged Molecular Sieves. *Can. J. Chem.* **1974**, 52 (20), 3523–3528.
- (35) Karger, K.; Ruthven, D. M. *Diffusion in Zeolites and Other Microporous Solids*; Wiley: New York, 1992.
- (36) Satterfield, C. N. *Heterogeneous Catalysis in Industrial Practice*, 2nd ed.; McGraw-Hill: New York, 1993.
- (37) Breck, D. W. *Zeolite Molecular Sieve Structure, Chemistry and Use*; Wiley: New York, 1974.
- (38) Habgood, H. W. Kinetics of molecular-sieve action. Sorption of nitrogen methane mixtures by Linde Molecular Sieve 4A. *Can. J. Chem.* **1958**, 36, 1384–97.
- (39) Qureshi, W. R.; Wei, J. One- and Two-Component Diffusion in Zeolite ZSM-5. *J. Catal.* **1990**, 126, 126–146.

Received for review September 16, 2004

Revised manuscript received January 19, 2005

Accepted February 3, 2005

IE049095U